Results in Physics 25 (2021) 104303

Contents lists available at ScienceDirect

Results in Physics

journal homepage: www.elsevier.com/locate/rinp

On the modulation instability analysis and deeper properties of the cubic nonlinear Schrödinger's equation with repulsive δ-potential

Yi-Xia Li [a], Ercan Celik [b], Juan L.G. Guirao [c,d,*], Tareq Saeed [d], Haci Mehmet Baskonus [e]

[a] College of Mathematics and Finance, Xiangnan University, Chenzhou 423000, PR China
[b] Faculty of Science, Department of Mathematics, Ataturk University, Erzurum, Turkey
[c] Technical University of Cartagena, Department of Applied Mathematics and Statistics, Cartagena, Spain
[d] Nonlinear Analysis and Applied Mathematics (NAAM)-Research Group, Department of Mathematics, Faculty of Science, King Abdulaziz University, P.O. Box 80203, Jeddah 21589, Saudi Arabia
[e] Faculty of Education, Department of Mathematics and Science Education, Harran University, Sanliurfa, Turkey

ARTICLE INFO

Keywords:
The cubic nonlinear Schrödinger's equation
The generalized exponential rational function method
Modulation instability analysis
Hyperbolic and dark bright soliton solutions

ABSTRACT

This projected work applies the generalized exponential rational function method to extract the complex, trigonometric, hyperbolic, dark bright soliton solutions of the cubic nonlinear Schrödinger's equation. Moreover, trigonometric, complex, strain conditions and dark-bright soliton wave distributions are also reported. Furthermore, the modulation instability analysis is also studied in detail. To better understand the dynamic behavior of some of the obtained solutions, several numerical simulations are presented in the paper. According to the obtained results, it is clear that the method has less limitations than other methods in determining the exact solutions of the equations. Despite the simplicity and ease of use of this method, it has a very powerful performance and is able to introduce a wide range of different types of solutions to such equations. The idea used in this paper is readily applicable to solving other partial differential equations in mathematical physics.

Introduction

In modern century, many experts from all over the world have directed their studies to the investigation of deep properties of nonlinear partial differential evaluations (NLPDEs). In this sense, nonlinear reaction-diffusion and wave-type equations with delay containing variable coefficients and arbitrary functions have been observed in [1]. Global stability analysis of a fractional SVEIR epidemic model has been presented in [2]. The fifth order potential Bogoyavlenskii-Schiff equation has been studied in a detailed manner in [3]. Some important properties of the fractional predator-prey-pathogen model with Mittag-Leffler kernel-based operators have been reported in [4]. By using the first integral method, several important roots of Wu-Zhang system with conformable have been archived in [5]. Second-order Sobolev-type impulsive neutral differential evolution inclusions with infinite delay has been investigated in detail [6]. Rational solutions, and the interaction solutions to the $(2+1)$-dimensional time-dependent Date-Jimbo-Kashiwara-Miwa equation have been observed in [7]. The Brusselator reaction-diffusion system arising in chemical reactions have been also introduced to the literature [8]. In modern century, some important studies of real world problems such as coronavirus [9–11], predator-prey [12–14], dispersive long wave [15], interaction of tumor growth and the immune system [16], film problems [17], edge detecting techniques [18], Fisher-KPP problems [19], the modeling hand-footmouth disease [20], the resonance nonlinear Schrödinger equation with intermodal dispersions [21], the extended nonlinear Schrödinger's equation [22], HIV/AIDS transmission model [23], Schamel's equation [24], Burgers' equation with time delay [25], integrodifferential equations with nonlocal conditions [26], Zakharov-Kuznetsov [27], Gardner's equation [28], generalized Gerdjikov-Ivanov equation [29] and Kawahara-KdV type equation [30] and so on [31–39] have been investigated in a detailed manner.

In this paper, we consider the cubic nonlinear Schrödinger's equation with repulsive delta potential as [40]

* Corresponding author at: Technical University of Cartagena, Department of Applied Mathematics and Statistics, Cartagena, Spain. Nonlinear Analysis and Applied Mathematics (NAAM)-Research Group, Department of Mathematics, Faculty of Science, King Abdulaziz University, P.O. Box 80203, Jeddah 21589, Saudi Arabia.

E-mail addresses: ercelik@atauni.edu.tr (E. Celik), Juan.Garcia@upct.es, jlgarcia@kau.edu.sa (J.L.G. Guirao), tsalmalki@kau.edu.sa (T. Saeed).

https://doi.org/10.1016/j.rinp.2021.104303
Received 17 March 2021; Received in revised form 18 April 2021; Accepted 7 May 2021
Available online 20 May 2021

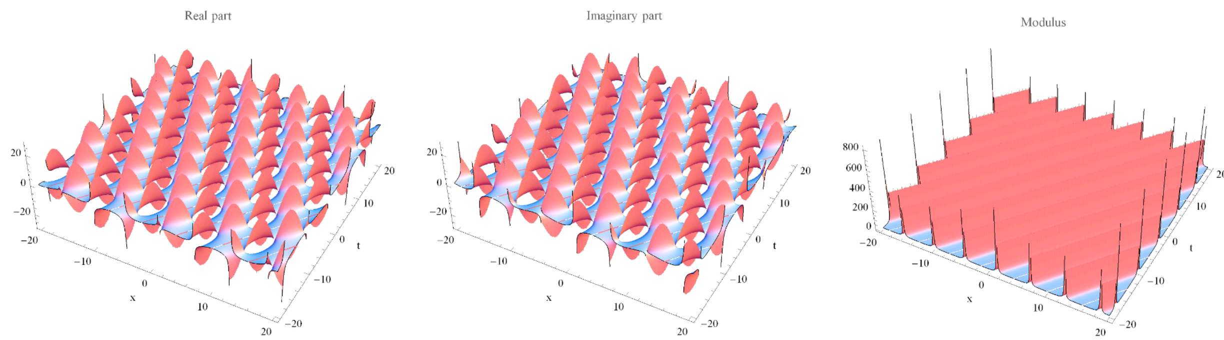

Fig. 1. 3D plot corresponding to the solution $u_1(x,t)$ in Eq. (10) when $A_0=1, a=0.2, b=0.3, \delta=0.1, r=0.3$.

$$i\frac{\partial\mathfrak{u}(x,t)}{\partial t}+\frac{1}{2}\frac{\partial^2\mathfrak{u}(x,t)}{\partial x^2}-a\delta\mathfrak{u}(x,t)-b|\mathfrak{u}(x,t)|^2\mathfrak{u}(x,t)=0, \tag{1}$$

where a and b are tow nonzero real constants, δ is the dirac measure at the origin. The soliton-defect interactions of Eq. (1) have been presented by Goodman et al. [41]. Eq. (1) is used to describe the resonant nonlinear propagation of light through optical wave guides with localized defects [42]. This governing model can be also investigated by using various methods such as the trigonometric function series method [48], the modified mapping method and the extended mapping method [49], the modified trigonometric function series method [50], the bifurcation method and qualitative theory of dynamical systems [51], the modified (G'/G)-expansion method [52], dynamical systems approach [53], the extended (G'/G)-expansion method [54] and so on [55–60]. Recently, many experts have immensely studied to investigate the deeper properties of mathematical models by using various approaches [62–77].

The outline of the method

As the theory of differential equations progresses, we need some new techniques to help us find exact solutions to such equations. One of these efficient methods is the generalized exponential rational function method (GERFM) [43]. This method has been used to solve many nonlinear models in mathematics and physics with many applications in science and technology [44–47]. This method should be used as follows.
.

1. First, let us assume that we are going to solve a nonlinear partial differential equation of the following form

$$\mathcal{N}(\mathfrak{u},\mathfrak{u}_x,\mathfrak{u}_t,\mathfrak{u}_{xx},\dots)=0. \tag{2}$$

Taking transformations $\mathfrak{u}=\mathfrak{u}(\xi)$ and $\xi=\sigma x-\varphi t$ into account in (2) reduces the problem to the following ordinary differential equation

$$\mathcal{N}(\mathfrak{u},\mathfrak{u}',\mathfrak{u}'',\dots)=0. \tag{3}$$

2. The main assumption of the method is based on the fact that the equation has a solution in the following symbolic form

$$\mathfrak{u}(\xi)=\alpha_0+\sum_{k=1}^{\kappa}\alpha_k\Theta(\xi)^k+\sum_{k=1}^{\kappa}\beta_k\Theta(\xi)^{-k}, \tag{4}$$

where

$$\Theta(\xi)=\frac{\rho_1e^{\theta_1\xi}+\rho_2e^{\theta_2\xi}}{\rho_3e^{\theta_3\xi}+\rho_4e^{\theta_4\xi}}. \tag{5}$$

Also, $\rho_i,\theta_i(1\leqslant i\leqslant 4),\alpha_0,\alpha_k$ and $\beta_k(1\leqslant k\leqslant\kappa)$ are unknown parameters which cause this solution to be satisfied in the equation. Moreover, κ is a balancing number of the equation.

3. Putting Eq. (4) into Eq. (3), a set of nonlinear system of algebraic equations is constructed based on the parameters in the solution.
4. By solving this nonlinear system of equations and placing its nontrivial solutions into the general form considered in (4), the solutions of the original equation are obtained.

Mathematical analysis

To investigate the exact solution of Eq. (1), let us define the following new transformations

$$\mathfrak{u}(x,t)=\mathfrak{u}(\xi)\times e^{i\Phi},\qquad \xi=\mu(x-\nu t),\Phi=px+rt. \tag{6}$$

where μ and k are unknown constants.

Taking Eq. (6) into account converts Eq. (1), from the imaginary part we find that $\nu=p$. Moreover the following ordinary differential equation is also obtained from the real part [42]

$$\mu^2\mathfrak{u}''(\xi)-2b\mathfrak{u}^3(\xi)-\left(p^2+2(r+a\delta)\right)\mathfrak{u}(\xi)=0. \tag{7}$$

This equation has also some properties of the Duffing equation which is the equation governing the oscillations of a mass attached to the end of a spring whose tension (or compression) [61]. Taking balance principles between $\mathfrak{u}^3$ and $\mathfrak{u}''$ into account in Eq. (7) yields $3\kappa=\kappa+2\rightarrowtail\kappa=1$. Immediately the general structure for the solution to the problem, which is presented in (4), is determined as follows

$$\mathfrak{u}(\xi)=\alpha_0+\alpha_1\Theta(\xi)+\beta_1\Theta^{-1}(\xi). \tag{8}$$

Following the steps mentioned for the method, the solutions of the equation will be specified as follows.

Class 1:

Taking $[\rho_1,\rho_2,\rho_3,\rho_4]=[1-i,1+i,1,1]$ and $[\theta_1,\theta_2,\theta_3,\theta_4]=[i,-i,i,-i]$ in Eq. (5) into account yields

$$\Theta(\xi)=\frac{\cos(\xi)+\sin(\xi)}{\cos(\xi)}. \tag{9}$$

Case 1: Other parameters, in this case, are as follows

$$\mu=A_0\sqrt{b},\nu=\sqrt{2A_0^2b-2a\delta-2r},r=r,A_0=A_0,A_1=0,B_1=-2A_0.$$

Substituting these solutions into (8) and (9), one achieves

$$\mathfrak{u}(\xi)=\frac{A_0(2\cos(\xi)\sin(\xi)-1)}{2(\cos(\xi))^2-1}.$$

Based on these results, we obtain the following solution

$$\mathrm{u}_1(x,t)=\frac{A_0\left(2\cos\left(A_0\sqrt{b}\left(-\sqrt{2A_0^2b-2a\delta-2r}\,t+x\right)\right)\sin\left(A_0\sqrt{b}\left(-\sqrt{2A_0^2b-2a\delta-2r}\,t+x\right)\right)-1\right)}{2\left(\cos\left(A_0\sqrt{b}\left(-\sqrt{2A_0^2b-2a\delta-2r}\,t+x\right)\right)\right)^2-1}\times e^{\mathrm{i}(\nu x+rt)}. \tag{10}$$

We have plotted the dynamic behavior of the solution $u_1(x,t)$ given by Eq. (10) in Fig. 1.

Case 2: Other parameters, in this case, are as follows

$$\mu=A_1\sqrt{b},\nu=\sqrt{2A_1^2b-2a\delta-2r},r=r,A_0=-A_1,A_1=A_1,B_1=0.$$

Substituting these solutions into (8) and (9), one achieves

$$\mathrm{u}(\xi)=\frac{A_1\sin(\xi)}{\cos(\xi)}.$$

Based on these results, we obtain the following solution

$$\mathrm{u}_2(x,t)=\frac{A_1\sin\left(A_1\sqrt{b}\left(-\sqrt{2A_1^2b-2a\delta-2r}\,t+x\right)\right)}{\cos\left(A_1\sqrt{b}\left(-\sqrt{2A_1^2b-2a\delta-2r}\,t+x\right)\right)}\times e^{\mathrm{i}(\nu x+rt)}. \tag{11}$$

Class 2:

Taking $[\rho_1,\rho_2,\rho_3,\rho_4]=[1-i,-1-i,-1,1]$ and $[\theta_1,\theta_2,\theta_3,\theta_4]=[i,-i,i,-i]$ in Eq. (5) into account yields

$$\Theta(\xi)=\frac{-\sin(\xi)+\cos(\xi)}{\sin(\xi)}. \tag{12}$$

Case 1: Other parameters, in this case, are as follows

$$\mu=A_0\sqrt{b},\nu=\sqrt{2A_0^2b-2a\delta-2r},r=r,A_0=A_0,A_1=0,B_1=2A_0.$$

Inserting these solutions into (8) and (12), it reads

$$\mathrm{u}(\xi)=\frac{A_0(\cos(\xi)+\sin(\xi))}{-\sin(\xi)+\cos(\xi)}.$$

Based on these results, one obtained the following exact solution

$$\mathrm{u}_3(x,t)=\frac{A_0\left(\cos\left(A_0\sqrt{b}\left(-\sqrt{2A_0^2b-2a\delta-2r}\,t+x\right)\right)+\sin\left(A_0\sqrt{b}\left(-\sqrt{2A_0^2b-2a\delta-2r}\,t+x\right)\right)\right)}{-\sin\left(A_0\sqrt{b}\left(-\sqrt{2A_0^2b-2a\delta-2r}\,t+x\right)\right)+\cos\left(A_0\sqrt{b}\left(-\sqrt{2A_0^2b-2a\delta-2r}\,t+x\right)\right)}\times e^{\mathrm{i}(\nu x+rt)}. \tag{13}$$

The dynamic behavior of the solution $u_3(x,t)$ given by Eq. (13) are displayed Fig. 2.

Case 2: Other parameters, in this case, are as follows

$$\mu=A_1\sqrt{b},\nu=\sqrt{2A_1^2b-2a\delta-2r},r=r,A_0=A_1,A_1=A_1,B_1=0.$$

Inserting these solutions into (8) and (12), it reads

$$\mathrm{u}(\xi)=\frac{A_1\cos(\xi)}{\sin(\xi)}.$$

Based on these results, one obtained the following exact solution

$$\mathrm{u}_4(x,t)=\frac{A_1\cos\left(\sqrt{b}\left(-\sqrt{2A_1^2b-2a\delta-2r}\,t+x\right)\right)}{\sin\left(A_1\sqrt{b}\left(-\sqrt{2A_1^2b-2a\delta-2r}\,t+x\right)\right)}\times e^{\mathrm{i}(\nu x+rt)}. \tag{14}$$

Class 3:

Taking $[\rho_1,\rho_2,\rho_3,\rho_4]=[2-i,-2-i,-1,1]$ and $[\theta_1,\theta_2,\theta_3,\theta_4]=[i,-i,i,-i]$ in Eq. (5) into account yields

$$\Theta(\xi)=\frac{-2\sin(\xi)+\cos(\xi)}{\sin(\xi)}. \tag{15}$$

Case 1: Other parameters, in this case, are as follows

$$\mu=A_0\sqrt{b},\nu=\sqrt{2A_0^2b-2a\delta-2r},r=r,A_0=A_0,A_1=0,B_1=5A_0.$$

Inserting these solutions into (8) and (15), it reads

$$\mathrm{u}(\xi)=\frac{A_0(2\cos(\xi)+\sin(\xi))}{-4\sin(\xi)+2\cos(\xi)}.$$

Based on these results, one obtained the following exact solution

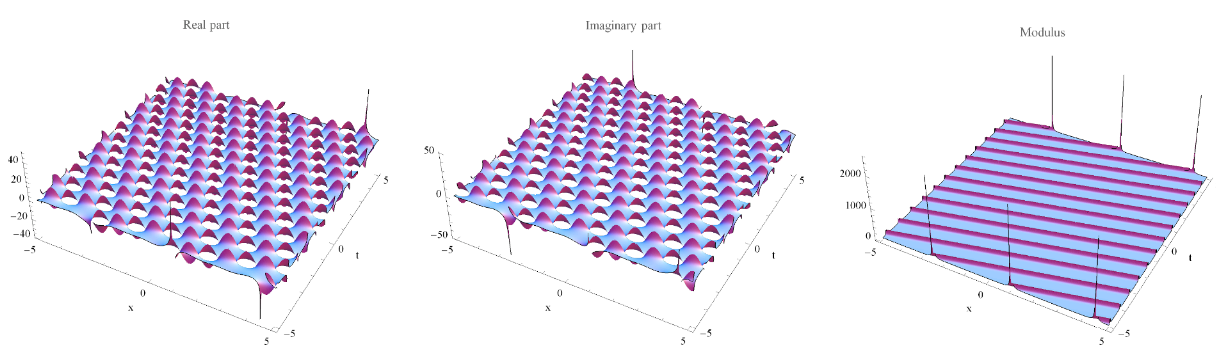

Fig. 2. 3D plot corresponding to the solution $u_3(x,t)$ in Eq. (13) when $A_0=1,a=2,b=0.8,\delta=-2,r=2$.

$$u_5(x,t) = \frac{A_0\left(2\cos\left(A_0\sqrt{b}\left(-\sqrt{2A_0^2b-2a\delta-2r}\,t+x\right)\right)+\sin\left(A_0\sqrt{b}\left(-\sqrt{2A_0^2b-2a\delta-2r}\,t+x\right)\right)\right)}{-4\sin\left(A_0\sqrt{b}\left(-,\sqrt{2A_0^2b-2a\delta-2r}\,t+x\right)\right)+2\cos\left(A_0\sqrt{b}\left(-\sqrt{2A_0^2b-2a\delta-2r}\,t+x\right)\right)}\times e^{i(\nu x+rt)}. \tag{16}$$

Class 4:

Taking $[\rho_1,\rho_2,\rho_3,\rho_4]=[-1,0,1,1]$ and $[\theta_1,\theta_2,\theta_3,\theta_4]=[0,0,1,0]$ in Eq. (5) into account yields

$$\Theta(\xi) = -\frac{1}{1+e^{\xi}}. \tag{17}$$

Case 1: Other parameters, in this case, are as follows

$$\mu=2A_0\sqrt{b}, \nu=\nu, r=-A_0^2b-a\delta-1\big/2\nu^2, A_0=A_0, A_1=2A_0, B_1=0.$$

Inserting these solutions into (8) and (17), it reads

$$u(\xi)=\frac{A_0(e^{\xi}-1)}{e^{\xi}+1}.$$

Based on these results, one obtained the following exact solution

$$u_6(x,t)=\frac{A_0\left(e^{2A_0\sqrt{b}(-\nu t+x)}-1\right)}{e^{2A_0\sqrt{b}(-\nu t+x)}+1}\times e^{i(\nu x+rt)}. \tag{18}$$

The dynamic behavior of the solution $u_6(x,t)$ given by Eq. (18) are displayed Fig. 3.

Class 5:

Taking $[\rho_1,\rho_2,\rho_3,\rho_4]=[3,2,1,1]$ and $[\theta_1,\theta_2,\theta_3,\theta_4]=[1,0,1,0]$ in Eq. (5) into account yields

$$\Theta(\xi)=\frac{3e^{\xi}+2}{e^{\xi}+1}. \tag{19}$$

Case 1: Other parameters, in this case, are as follows

$$\mu=2A_0\sqrt{b}, \nu=\sqrt{-2A_0^2b-2a\delta-2r}, r=r, A_0=A_0, A_1=0, B_1=-12A_0.$$

Inserting these solutions into (8) and (19), it reads

$$u(\xi)=\frac{A_0(3e^{\xi}-2)}{15e^{\xi}+10}.$$

Based on these results, one obtained the following exact solution

$$u_7(x,t)=\frac{A_0\left(3e^{2A_0\sqrt{b}\left(\sqrt{-2A_0^2b-2a\delta-2r}\,t+x\right)}-2\right)}{15e^{2A_0\sqrt{b}\left(-\sqrt{-2A_0^2b-2a\delta-2r}\,t+x\right)}+10}\times e^{i(\nu x+rt)}. \tag{20}$$

The dynamic behavior of the solution $u_7(x,t)$ given by Eq. (20) are displayed Fig. 4.

Taking $[\rho_1,\rho_2,\rho_3,\rho_4]=[-1,1,1,1]$ and $[\theta_1,\theta_2,\theta_3,\theta_4]=[1,-1,1,-1]$ in Eq. (5) into account yields

$$\Theta(\xi)=-\frac{\sinh(\xi)}{\cosh(\xi)}. \tag{21}$$

Case 1: Other parameters, in this case, are as follows

$$\mu=A_1\sqrt{b}, \nu=\sqrt{4A_1^2b-2a\delta-2r}, r=r, A_0=0, A_1=A_1, B_1=-A_1.$$

Inserting these solutions into (8) and (21), it reads

$$u(\xi)=\frac{A_1}{\cosh(\xi)\sinh(\xi)}.$$

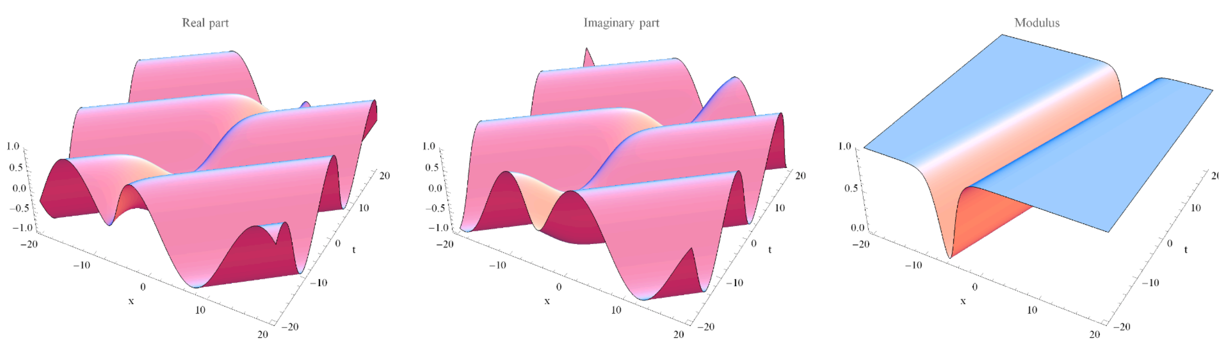

Fig. 3. 3D plot corresponding to the solution $u_6(x,t)$ in Eq. (18) when $A_0=1, a=0.2, b=0.3, \delta=0.1, \nu=0.3$.

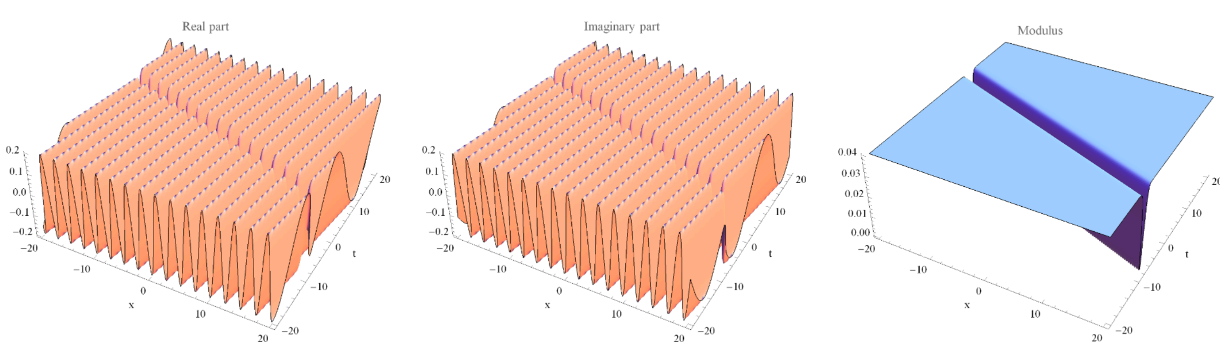

Fig. 4. 3D plot corresponding to the solution $u_7(x,t)$ in Eq. (20) when $A_0=1, a=2, b=0.5, \delta=-2, r=0.3$.

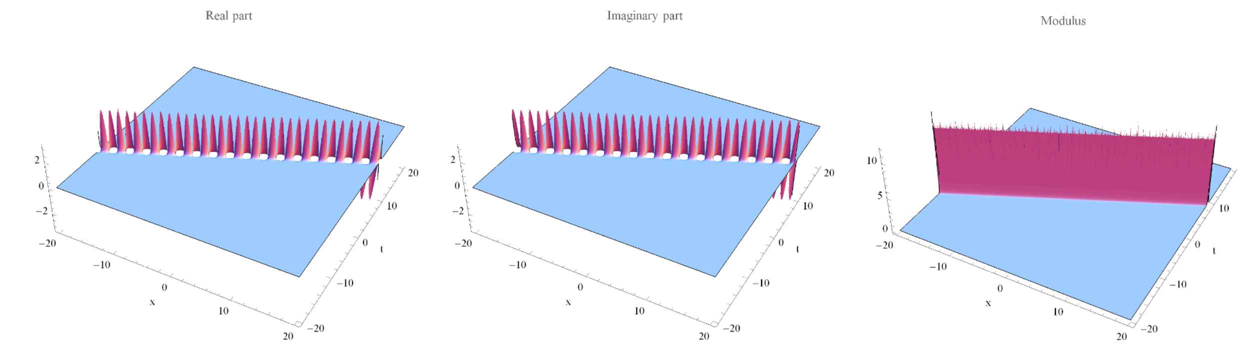

Fig. 5. 3D plot corresponding to the solution $u_8(x,t)$ in Eq. (22) when $A_1=1, a=1.3, b=2, \delta=0.5, r=0.9$.

Based on these results, one obtained the following exact solution

$$u_8(x,t)=\frac{A_1}{\cosh\left(A_1\sqrt{b}\left(-\sqrt{4A_1^2b-2a\delta-2r}\,t+x\right)\right)\sinh\left(A_1\sqrt{b}\left(-\sqrt{4A_1^2b-2a\delta-2r}\,t+x\right)\right)}\times e^{\mathrm{i}(\nu x+rt)}. \tag{22}$$

The dynamic behavior of the solution $u_8(x,t)$ given by Eq. (22) are displayed Fig. 5.

Class 7:

Taking $[\rho_1,\rho_2,\rho_3,\rho_4]=[-2-i,2-i,-1,1]$ and $[\theta_1,\theta_2,\theta_3,\theta_4]=[i,-i,i,-i]$ in Eq. (5) into account yields

$$\Theta(\xi)=\frac{\cos(\xi)+2\sin(\xi)}{\sin(\xi)}. \tag{23}$$

Case 1: Other parameters, in this case, are as follows

$$\mu=A_0\sqrt{b}, \nu=\sqrt{2A_0^2b-4a\delta-4r}, r=r, A_0=A_0, A_1=0, B_1=-5\Big/2A_0.$$

Inserting these solutions into (8) and (23), it reads

$$u(\xi)=\frac{A_0(-\sin(\xi)+2\cos(\xi))}{2\cos(\xi)+4\sin(\xi)}.$$

Based on these results, one obtained the following exact solution

$$u_9(x,t)=\frac{A_0\left(-\sin\left(A_0\sqrt{b}\left(-\sqrt{2A_0^2b-2a\delta-2r}\,t+x\right)\right)+2\cos\left(A_0\sqrt{b}\left(-\sqrt{2A_0^2b-2a\delta-2r}\,t+x\right)\right)\right)}{2\cos\left(A_0\sqrt{b}\left(-\sqrt{2A_0^2b-2a\delta-2r}\,t+x\right)\right)+4\sin\left(A_0\sqrt{b}\left(-\sqrt{2A_0^2b-3a\delta-2r}\,t+x\right)\right)}\times e^{\mathrm{i}(\nu x+rt)}. \tag{24}$$

Class 8:

Taking $[\rho_1,\rho_2,\rho_3,\rho_4]=[-3,-1,1,1]$ and $[\theta_1,\theta_2,\theta_3,\theta_4]=[1,-1,1,-1]$ in Eq. (5) into account yields

$$\Theta(\xi)=\frac{-2\cosh(\xi)-\sinh(\xi)}{\cosh(\xi)}. \tag{25}$$

Case 1: Other parameters, in this case, are as follows

$$\mu=A_0\sqrt{b}, \nu=\sqrt{-2A_0^2b-2a\delta-2r}, r=r, A_0=A_0, A_1=0, B_1=3A_0.$$

Inserting these solutions into (8) and (25), it reads

$$u(\xi)=\frac{A_0(2\sinh(\xi)+\cosh(\xi))}{4\cosh(\xi)+2\sinh(\xi)}.$$

Based on these results, one obtained the following exact solution

$$u_{10}(x,t)=\frac{A_0\left(2\sinh\left(A_0\sqrt{b}\left(-\sqrt{-2A_0^2b-2a\delta-2r}\,t+x\right)\right)+\cosh\left(A_0\sqrt{b}\left(-\sqrt{-2A_0^2b-2a\delta-2r}\,t+x\right)\right)\right)}{4\cosh\left(A_0\sqrt{b}\left(-\sqrt{-2A_0^2b-2a\delta-2r}\,t+x\right)\right)+2\sinh\left(A_0\sqrt{b}\left(-\sqrt{-2A_0^2b-2a\delta-2r}\,t+x\right)\right)}\times e^{\mathrm{i}(\nu x+rt)}. \tag{26}$$

The dynamic behavior of the solution $u_{10}(x,t)$ given by Eq. (26) are displayed Figs. 6 and 7.

Class 9:

Taking $[\rho_1,\rho_2,\rho_3,\rho_4]=[i,-i,1,1]$ and $[\theta_1,\theta_2,\theta_3,\theta_4]=[i,-i,i,-i]$ in Eq. (5) into account yields

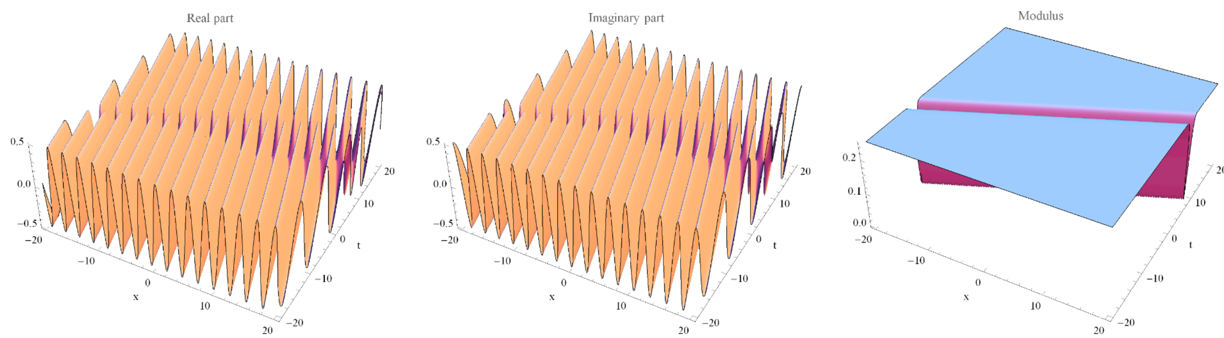

Fig. 6. 3D plot corresponding to the solution $u_{10}(x,t)$ in Eq. (26) when $A_0=1, a=4.2, b=2, \delta=-3.5, r=0.2$.

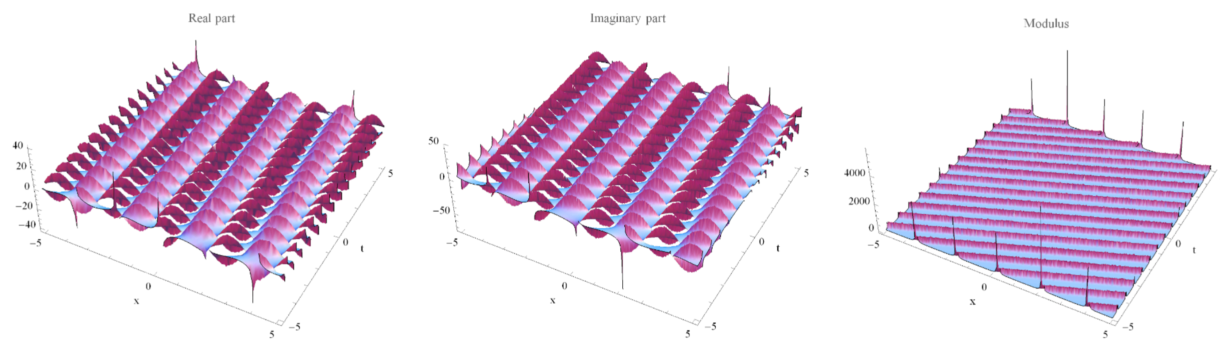

Fig. 7. 3D plot corresponding to the solution $u_{11}(x,t)$ in Eq. (26) when $B_1=1, a=1.2, b=0.7, \delta=-0.6, r=0.2$.

$$\Theta(\xi)=-\frac{\sin(\xi)}{\cos(\xi)}. \tag{27}$$

Case 1: Other parameters, in this case, are as follows

$$\mu=\sqrt{b}B_1, \nu=\sqrt{8B_1^2b-2a\delta-2r}, r=r, A_0=0, A_1=-B_1, B_1=B_1.$$

Inserting these solutions into (8) and (27), it reads

$$\mathfrak{u}(\xi)=\frac{B_1(1-2\cos^2(\xi))}{\cos(\xi)\sin(\xi)}.$$

Based on these results, one obtained the following exact solution

$$\mathfrak{u}_{11}(x,t)=\frac{B_1\left(1-2\cos^2\left(\sqrt{b}B_1\left(-\sqrt{8B_1^2b-2a\delta-2r}\,t+x\right)\right)\right)}{\cos\left(\sqrt{b}B_1\left(-\sqrt{8B_1^2b-2a\delta-2r}\,t+x\right)\right)\sin\left(\sqrt{b}B_1\left(-\sqrt{8B_1^2b-2a\delta-2r}\,t+x\right)\right)}\times e^{\mathrm{i}(\nu x+rt)}. \tag{28}$$

The dynamic behavior of the solution $u_{11}(x,t)$ given by Eq. (28) are displayed Fig. 6.

Class 10:

Taking $[\rho_1,\rho_2,\rho_3,\rho_4]=[i,-i,1,1]$ and $[\theta_1,\theta_2,\theta_3,\theta_4]=[i,-i,i,-i]$ in Eq. (5) into account yields

$$\Theta(\xi)=\frac{-e^{\xi}-2}{e^{\xi}+1}. \tag{29}$$

Case 1: Other parameters, in this case, are as follows

$$\mu=2A_0\sqrt{b}, \nu=\sqrt{-2A_0^2b-2a\delta-2r}, r=r, A_0=A_0, A_1=0, B_1=4A_0.$$

Inserting these solutions into (8) and (29), it reads

$$\mathfrak{u}(\xi)=-\frac{A_0(e^{\xi}-2)}{3e^{\xi}+6}.$$

Based on these results, one obtained the following exact solution

$$\mathfrak{u}_{12}(x,t)=-\frac{A_0\left(e^{2A_0\sqrt{b}\left(-\sqrt{-2A_0^2b-2a\delta-2r}\,t+x\right)}-2\right)}{3e^{2A_0\sqrt{b}\left(-\sqrt{-2A_0^2b-2a\delta-2r}\,t+x\right)}+6}\times e^{\mathrm{i}(\nu x+rt)}. \tag{30}$$

Modulation instability analysis

In this section of the article we discuss instability modulation analysis (MI) for the stationary solutions of Eq. (1) by assuming that Eq. (1) have the following stationary solutions

$$u(x,t)=(\sqrt{P_0}+\rho(x,t))e^{i\phi}, \phi=P_0x \tag{31}$$

where P_0 represent the incident power. We investigate the evolution of the perturbation $\rho(x,t)$ using the concept of linear stability analysis. Substituting Eq. (31) into Eq. (1) and linearizing the result in $\rho(x,t)$, we acquire.

$$i\rho_t+\frac{1}{2}\rho_{xx}-a\delta(\sqrt{P_0}+\rho)-bP_0(\rho+\rho*)=0, \tag{32}$$

where $\rho*$ is the conjugate function, supposing solutions of Eq. (32) are in the following

$$\rho(x,t)=\gamma e^{i(\beta x-\alpha t)}+\delta e^{-i(\beta x-\alpha t)}, \tag{33}$$

where β is the wave number, α is the frequency of the perturbation.

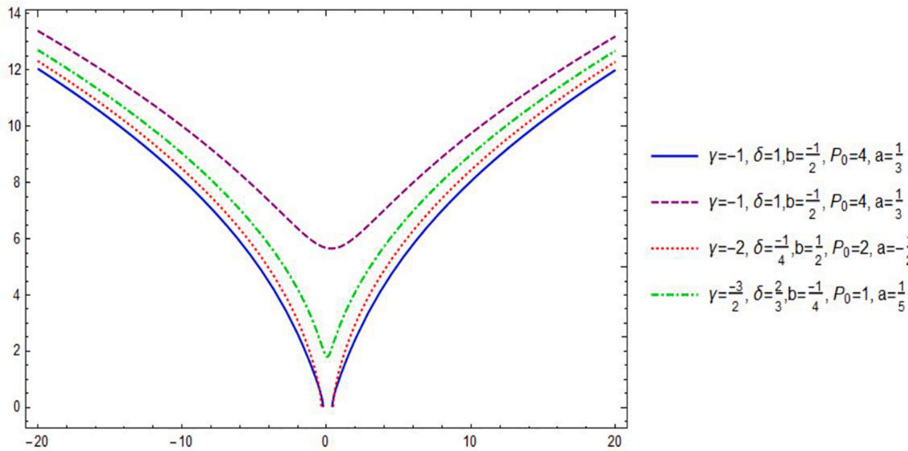

Fig. 8. The instability modulation for different values mentioned parameters.

Putting Eq. (33) in Eq. (32) gives a set of two homogenous equations as follows

$$\alpha\gamma\frac{1}{2}\beta^2\gamma-\alpha\gamma\beta-a\delta\sqrt{P_0}-b\gamma P_0-b\tau P_0=0, \tag{34}$$

$$-b\gamma P_0+\alpha\tau-\frac{1}{2}\beta^2\tau-a\delta\tau-b\tau P_0=0. \tag{35}$$

From Eqs. (34,35) one can easily obtain the following coefficient matrix of γ and τ .

$$\begin{pmatrix} -\alpha-\frac{1}{2}\beta^2-a\delta-\frac{1}{\gamma}a\delta\sqrt{P_0}-bP_0 & -bP_0 \\ -bP_0 & \alpha-\frac{1}{2}\beta^2-a\delta-bP_0 \end{pmatrix}\begin{pmatrix}\gamma\\ \tau\end{pmatrix}=\begin{pmatrix}0\\0\end{pmatrix}. \tag{36}$$

The coefficient matrix in Eq. (36) has a nontrivial solution if the determinant equal to zero. By expanding the determinant, we obtain the following

$$\frac{\gamma(-4\alpha^2+(\beta^2+2a\delta)^2)+2a\delta(-2\alpha+\beta^2+2a\delta)\sqrt{P_0}+4b\gamma(\beta^2+2a\delta)P_0+4ab\delta P_0^{\frac{3}{2}}}{4\gamma}=0. \tag{37}$$

Eq. (37) has the following solutions

$$\beta=\mp\sqrt{-\frac{a\delta(2\gamma+\sqrt{P_0})+2b\gamma P_0+\sqrt{4\alpha^2\gamma^2+4a\alpha\gamma\delta\sqrt{P_0}+a^2\delta^2P_0+4b^2\gamma^2P_0^2)}}{\gamma}}. \tag{38}$$

$$\beta=\mp\sqrt{\frac{-a\delta(2\gamma+\sqrt{P_0})-2b\gamma P_0+\sqrt{4\alpha^2\gamma^2+4a\alpha\gamma\delta\sqrt{P_0}+a^2\delta^2P_0+4b^2\gamma^2P_0^2)}}{\gamma}}. \tag{39}$$

The stability of the steady state is determined by Eqs. (38,39). If the wave number β has an imaginary part, the steady-state solution is unstable since the perturbation grows exponentially. But if the wave number β is real, the steady state is stable against small perturbation. Thus, the necessary condition for the existence of modulation instability to occur from Eqs. (38,39) is when either

$$\frac{a\delta(2\gamma+\sqrt{P_0})+2b\gamma P_0+\sqrt{4\alpha^2\gamma^2+4a\alpha\gamma\delta\sqrt{P_0}+a^2\delta^2P_0+4b^2\gamma^2P_0^2)}}{\gamma}>0, \tag{40}$$

or

$$\frac{-a\delta(2\gamma+\sqrt{P_0})-2b\gamma P_0+\sqrt{4\alpha^2\gamma^2+4a\alpha\gamma\delta\sqrt{P_0}+a^2\delta^2P_0+4b^2\gamma^2P_0^2)}}{\gamma}<0. \tag{41}$$

Now for investigating instability modulation gain spectrum it should be noticed that

$$g(\alpha)=2Im(\beta)=\mp2\sqrt{\frac{a\delta(2\gamma+\sqrt{P_0})+2b\gamma P_0+\sqrt{4\alpha^2\gamma^2+4a\alpha\gamma\delta\sqrt{P_0}+a^2\delta^2P_0+4b^2\gamma^2P_0^2)}}{\gamma}}>0, \tag{42}$$

It must be taking to consideration that $\gamma\neq0$, we have the following cases.

Case 1) If

$$g(\alpha)=2Im(\beta)=2\sqrt{\frac{a\delta(2\gamma+\sqrt{P_0})+2b\gamma P_0+\sqrt{4\alpha^2\gamma^2+4a\alpha\gamma\delta\sqrt{P_0}+a^2\delta^2P_0+4b^2\gamma^2P_0^2)}}{\gamma}}>0, \tag{43}$$

we have the following sub cases

Case 1.1) For these values $\gamma=\frac{-2}{3}, \delta=\frac{2}{5}, b=2, P_0=1, a=\frac{1}{4}$,of constants in Eq. (43) we have

$$g_{1,1}(\alpha)=\frac{\sqrt{-81+\sqrt{6409+80\alpha(-3+20\alpha)}}}{\sqrt{5}}, \tag{44}$$

Case 1.2) When $\gamma=-1, \delta=1, b=\frac{-1}{2}, P_0=4, a=\frac{1}{3}$in Eq. (43), we find

$$g_{1,2}(\alpha)=2\sqrt{4+\sqrt{\frac{148}{9}-\frac{8\alpha}{3}+4\alpha^2}}, \tag{45}$$

Case 1.3) Selecting $\gamma=-2, \delta=-\frac{1}{4}, b=\frac{1}{2}, P_0=2, a=-\frac{1}{2}$in Eq. (43), we extract

$$g_{1,3}(\alpha) = \frac{1}{2}\sqrt{-36 + \sqrt{2} + \sqrt{1026 + 64\alpha(-\sqrt{2} + 16\alpha)}}, \tag{46}$$

Case 1.4) Taking as $\gamma = -\frac{3}{2}, \delta = \frac{2}{3}, b = \frac{-1}{4}, P_0 = 1, a = \frac{1}{5}$ in Eq. (43), we gain the following solution

$$g_{1,4}(\alpha) = \frac{1}{3}\sqrt{\frac{2}{5}}\sqrt{29 + \sqrt{2089 + 72\alpha(-4 + 45\alpha)}}. \tag{47}$$

These sub cases can be expressed as the following graphs.

Conclusions

In this worked manuscript, we have studied on the application of GERFM to the cubic nonlinear Schrödinger's equation with repulsive delta potential. Many entirely new analytical solutions such as trigonometric and hyperbolic function solutions, dark-bright soliton solutions and also modulus properties to the governing model have been also reported. Moreover, real and imaginary surfaces of solutions obtained have been simulated in detail. Strain conditions and modulation instability analysis according to findings have been also reported. It can be also seen that the results of the governing model demonstrates the various types of wave propagations such as travelling and periodic wave distributions in physical problems. Travelling wave solutions in Figs. 1, 2, 3, 4, 6, 7 have been simulated while singular soliton solution has been also plotted in Fig. 5. Finally, the modulation instability analysis simulations has been also plotted in Fig. 8.

Funding

Not applicable.

Contributions

The authors read and approved the final version of the current paper.

Declaration of Competing Interest

The authors declare that they have no known competing financial interests or personal relationships that could have appeared to influence the work reported in this paper.

Acknowledgements

Fundación Séneca (Spain), grant 20783/PI/18., and Ministry of Science, Innovation and Universities (Spain), grant PGC2018-097198-B-100. Moreoer, this projected work was partially (not financial) supported by Harran University with the project HUBAP ID:20124.

References

[1] Polyanin AD, Sorokin VG. A method for constructing exact solutions of nonlinear delay PDEs. J Math Anal Appl 2021;494(2):124619.
[2] Nabti A, Ghanbari B. Global stability analysis of a fractional SVEIR epidemic model. Math Methods Appl Sci 2021. https://doi.org/10.1002/mma.7285.
[3] Wang WB, Lou GW, Shen XM, Song JQ. Exact solutions of various physical features for the fifth order potential Bogoyavlenskii-Schiff equation. Results Phys 2020;1(18):103243.
[4] Ghanbari B, Kumar S. A study on fractional predator-prey-pathogen model with Mittag-Leffler kernel-based operators. Numer Methods Partial Differ Eqs 2021.https://doi.org/10.1002/num.22689.
[5] Eslami M, Rezazadeh H. The first integral method for Wu-Zhang system with conformable time-fractional derivative. Calcolo 2016;53(3):475–85.
[6] Vijayakumar V, Panda SK, Nisar KS, Baskonus HM. Results on approximate controllability results for second-order Sobolev-type impulsive neutral differential evolution inclusions with infinite delay. Numer Methods Partial Differ Eqs 2021;37(2):1200–21.
[7] Ismael HF, Seadawy A, Bulut H. Rational solutions, and the interaction solutions to the (2+ 1)-dimensional time-dependent Date-Jimbo-Kashiwara-Miwa equation. Int J Comput Math 2021;1–9.
[8] Jena RM, Chakraverty S, Rezazadeh H, Domiri Ganji D. On the solution of time-fractional dynamical model of Brusselator reaction-diffusion system arising in chemical reactions. Math Methods Appl Sci 2020;43(7):3903–13.
[9] Gao W, Baskonus HM, Shi L. New investigation of bats-hosts-reservoir-people coronavirus model and application to 2019-nCoV system. Adv Differ Eqs 2020;2020(1):1.
[10] Gao W, Veeresha P, Baskonus HM, Prakasha DG, Kumar P.A new study of unreported cases of 2019-nCOV epidemic outbreaks. Chaos Solitons Fractals 2020;138:109929.
[11] Erturk VS, Kumar P. Solution of a COVID-19 model via new generalized Caputo-type fractional derivatives. Chaos Solitons Fractals 2020;1(139):110280.
[12] Ghanbari B, Djilali S. Mathematical and numerical analysis of a three-species predator-prey model with herd behavior and time fractional-order derivative. Math Methods Appl Sci 2020;43(4):1736–52.
[13] Ghanbari B. On approximate solutions for a fractional prey-predator model involving the Atangana-Baleanu derivative. Adv Differ Eqs 2020;2020(1):1–24.
[14] Djilali S, Ghanbari B. The influence of an infectious disease on a prey-predator model equipped with a fractional-order derivative. Adv Differ Eqs 2021;2021(1):1–6.
[15] Alharbi A, Almatrafi MB. Numerical investigation of the dispersive long wave equation using an adaptive moving mesh method and its stability. Results Phys 2020;1(16):102870.
[16] Ghanbari B. On the modeling of the interaction between tumor growth and the immune system using some new fractional and fractional-fractal operators. Adv Differ Eqs 2020;2020(1):1–32.
[17] Gao W, Veeresha P, Prakasha DG, Baskonus HM. New numerical simulation for fractional Benney-Lin equation arising in falling film problems using two novel techniques. Numer Methods Partial Differ Eqs 2021;37(1):210–43.
[18] Ghanbari B, Atangana A. Some new edge detecting techniques based on fractional derivatives with non-local and non-singular kernels. Adv Differ Eqs 2020;2020(1):1–9.
[19] McCue SW, El-Hachem M, Simpson MJ. Exact sharp-fronted travelling wave solutions of the Fisher-KPP equation. Appl Math Lett 2021;1(114):106918.
[20] Ghanbari B. A fractional system of delay differential equation with nonsingular kernels in modeling hand-foot-mouth disease. Advances in Difference Eqs 2020;2020(1):1-20.
[21] M. Srivastava H, Günerhan H, Ghanbari B. Exact traveling wave solutions for resonance nonlinear Schrödinger equation with intermodal dispersions and the Kerr law nonlinearity. Math Methods Appl Sci 2019;42(18):7210-21.
[22] Ghanbari B, Nisar KS, Aldhaifallah M. Abundant solitary wave solutions to an extended nonlinear Schrödinger's equation with conformable derivative using an efficient integration method. Adv Differ Eqs 2020;2020(1):1–25.
[23] Goyal M, Baskonus HM, Prakash A. Regarding new positive, bounded and convergent numerical solution of nonlinear time fractional HIV/AIDS transmission model. Chaos Solitons Fractals 2020;1(139):110096.
[24] Ghanbari B. On the nondifferentiable exact solutions to Schamel's equation with local fractional derivative on Cantor sets. Numer Methods Partial Differ Eqs 2021. https://doi.org/10.1002/num.22740.
[25] Herron I, McCalla C, Mickens R. Traveling wave solutions of Burgers' equation with time delay. Appl Math Lett 2020;1(107):106496.
[26] Munusamy K, Ravichandran C, Nisar KS, Ghanbari B. Existence of solutions for some functional integrodifferential equations with nonlocal conditions. Math Methods Appl Sci 2020;43(17):10319–31.
[27] Ghanbari B, Yusuf A, Baleanu D. The new exact solitary wave solutions and stability analysis for the (2+ 1) (2+ 1))dimensional Zakharov-Kuznetsov equation. Adv Differ Eqs 2019;2019(1):1–5.
[28] Ghanbari B. On novel nondifferentiable exact solutions to local fractional Gardner's equation using an effective technique. Numer Methods Partial Differ Eqs 2021. https://doi.org/10.1002/mma.7060.
[29] Kudryashov NA. Traveling wave solutions of the generalized Gerdjikov-Ivanov equation. Optik 2020;1(219):165193.
[30] Ghanbari B, Kumar S, Niwas M, Baleanu D. The Lie symmetry analysis and exact Jacobi elliptic solutions for the Kawahara-KdV type equations. Results Phys 2021;104006.
[31] Cattani Carlo, Sulaiman Tukur Abdulkadir, Baskonus Haci Mehmet, Bulut Hasan. On the soliton solutions to the Nizhnik-Novikov-Veselov and the Drinfel'd-Sokolov systems. Opt Quantum Electron 2018;50(3):138.
[32] Ismael HF, Bulut H, Baskonus HM. Optical soliton solutions to the Fokas-Lenells equation via sine-Gordon expansion method and (m+(G/G)-expansion method. Pramana 2019;94(1):1–9.
[33] Gao W, Yel G, Baskonus HM. C Cattani Complex Solitons in the Conformable (2+ 1)-dimensional Ablowitz-Kaup-Newell-Segur Equation. AIMS Math 2020;5(1):507–21.
[34] Gao W, Ismael HF, Bulut H, Baskonus HM. Instability modulation for the (2+ 1)-dimension paraxial wave equation and its new optical soliton solutions in Kerr media. Physica Scr 2020;95:035207.
[35] Esen A, Sulaiman TA, Bulut H, Baskonus HM. Optical solitons to the space-time fractional (1+ 1)-dimensional coupled nonlinear Schrödinger equation. Optik 2018;167:150–6.
[36] Atangana A. Fractional discretization: the African's tortoise walk. Chaos Solitons Fractals 2020;130:109399.
[37] Riaz MB, Atangana A, Jhangeer A, Tahir S. Soliton solutions, soliton-type solutions and rational solutions for the coupled nonlinear Schrödinger equation in magneto-optic waveguides. Eur Phys J Plus 2021;136(2):1–19.
[38] Atangana A. Blind in a commutative world: simple illustrations with functions and chaotic attractors. Chaos Solitons Fractals 2018;114:347–63.

[39] Atangana A. Fractal-fractional differentiation and integration: connecting fractal calculus and fractional calculus to predict complex system. Chaos Solitons Fractals 2017;102:396–406.
[40] Deift P, Park J. Long-time asymptotics for solutions of the NLS equation with a delta potential and even initial data. Int Math Res Notices 2011;2011(24): 5505–624.
[41] Goodman RH, Holmes PJ, Weinstein MI. Strong NLS soliton-defect interactions. Physica D 2004;192(3–4):215–48.
[42] Baskonus HM, Sulaiman TA, Bulut H, Aktürk T. Investigations of dark, bright, combined dark-bright optical and other soliton solutions in the complex cubic nonlinear Schrödinger equation with -potential. Superlattices Microstruct 2018;1 (115):19–29.
[43] Ghanbari B, Inc M. A new generalized exponential rational function method to find exact special solutions for the resonance nonlinear Schrödinger equation. Eur Phys J Plus 2018;133:1–19.
[44] Ghanbari B, Kuo CK. Abundant wave solutions to two novel KP-like equations using an effective integration method. Phys Scr 2021;96(4):045203.
[45] Ghanbari B, Günerhan H, Ílhan OA, Baskonus HM. Some new families of exact solutions to a new extension of nonlinear Schrödinger equation. Phys Scr 2020;95 (7):075208.
[46] Ghanbari B, Akgül A. Abundant new analytical and approximate solutions to the generalized Schamel equation. Phys Scr 2020;95(7):075201.
[47] Kumar S, Niwas M, Hamid I. Lie symmetry analysis for obtaining exact soliton solutions of generalized Camassa-Holm-Kadomtsev-Petviashvili equation. Int J Modern Phys B 2021;35(02):2150028.
[48] Zhang Z. New exact traveling wave solutions for the nonlinear Klein-Gordon equation. Turkish J Phys 2008;32(2008):235–40.
[49] Zhang Z, Liu Z, Miao X, Chen Y. New exact solutions to the perturbed nonlinear Schrodingers equation with Kerr law nonlinearity. Appl Math Comput 2010;216: 3064–72.
[50] Zhang Z, Li Y, Liu Z, Miao X. New exact solutions to the perturbed nonlinear Schrodingers equation with Kerr law nonlinearity via modified trigonometric function series method. Commun Nonlinear Sci Numer Simul 2011;16(8): 3097–3106.
[51] Zhang Z, Liu Z, Miao X, Chen Y. Qualitative analysis and traveling wave solutions for the perturbed nonlinear Schrodingers equation with Kerr law nonlinearity. Phys Lett A 2011;375:1275–80.
[52] Miao X, Zhang Z. The modified (G'/G)-expansion method and traveling wave solutions of nonlinear the perturbed nonlinear Schrodingers equation with Kerr law nonlinearity. Commun Nonlinear Sci Numer Simul 2011;16(11):4259–67.
[53] Zhang Z, Gan XY, Yu DM. Bifurcation behavior of the traveling wave solutions of nonlinear the perturbed nonlinear Schrodingers equation with Kerr law nonlinearity. Z Naturforschung A 2011. https://doi.org/10.5560/zna.2011-0041, 66(12).
[54] Zhang Z, Huang J, Zhong J, Dou SS, Liu J, Peng D, Gao T. The extended (G'/G)-expansion method and travelling wave solutions for the perturbed nonlinear Schrodingers equation with Kerr law nonlinearity. Pramana 2014;82(6):1011–29.
[55] Zhang Z, Wu J. Generalized (G'/G)-expansion method and exact traveling wave solutions of the perturbed nonlinear Schrödinger's equation with Kerr law nonlinearity in optical fiber materials. Opt Quantum Electron 2017;49(52):1–12.
[56] Zhang Z, Zhong J, Dou SS, Liu J, Peng D, Gao T. Abundant exact traveling wave solutions for the Klein-Gordon-Zakharov equations via the tanh-coth expansion method and Jacobi elliptic function expansion method. Rom J Phys 2013;58(7–8): 749–65.
[57] Zhang Z. First integral method and exact solutions to nonlinear partial differential equations arising in mathematical physics. Rom Rep Phys 2013;65(4):1155–69.
[58] Zhang Z. Jacobi elliptic function expansion method for the mKdVZK and the Hirota equations. Rom J Phys 2015;60(9–10):1384–94.
[59] Zhang Z. Exact traveling wave solutions of the perturbed Klein-Gordon equation with quadratic nonlinearity in (1+1)-dimension, Part I-without local inductance and dissipation effect. Turk J Phys 2013;37:259–67.
[60] Zhang Z, Zhong J, Dou SS, Liu J, Peng D, Gao T. A new method to construct traveling wave solutions for the Klein-Gordon Zakharov equations. Rom J Phys 2013;58(7–8):766–77.
[61] Zhang Z, Gan XY, Yu DM, Zhang YH, Li XP. A note on exact traveling wave solutions of the perturbed nonlinear Schrödinger's equation with Kerr law nonlinearity. Commun Theor Phys 2012;57(5):764.
[62] Cordero A, Jaiswal JP, Torregrosa JR. Stability analysis of fourth-order iterative method for finding multiple roots of non-linear equations. Appl Math Nonlinear Sci 2019;4(1):43–56.
[63] Eskitascioglu EI, Aktas MB, Baskonus HM. New complex and hyperbolic forms for Ablowitz-Kaup-Newell-Segur wave equation with fourth order. Appl Math Nonlinear Sci 2019;4(1):105–12.
[64] Houwe A, Sabiu J, Hammouch Z, Doka SY. Solitary pulses of a conformable nonlinear differential equation governing wave propagation in low-pass electrical transmission line. Phys Scr 2020;95(4):045203.
[65] Uddin MF, Hafez MG, Hammouch Z, Baleanu D. Periodic and rogue waves for Heisenberg models of ferromagnetic spin chains with fractional beta derivative evolution and obliqueness. Waves Random Complex Media 2020:1–15.
[66] Durur H, Yokus A. Exact solutions of (2+1)-Ablowitz-Kaup-Newell-Segur equation. Appl Math Nonlinear Sci 2020. https://doi.org/10.2478/amns.2020.2.00074.
[67] Aksoy NY. The solvability of first type boundary value problem for a Schrödinger equation. Appl Math Nonlinear Sci 2020;5(1):211–20.
[68] Arslan D. The comparison study of hybrid method with RDTM for solving Rosenau-Hyman equation. Appl Math Nonlinear Sci 2020;5(1):267–74.
[69] Arslan D. The numerical study of a hybrid method for solving telegraph equation. Appl Math Nonlinear Sci 2020;5(1):293–302.
[70] Uddin MF, Hafez MG, Hammouch Z, Rezazadeh H, Baleanu D. Traveling wave with beta derivative spatial-temporal evolution for describing the nonlinear directional couplers with metamaterials via two distinct methods. Alexandria Eng J 2021;60 (1):1055–65.
[71] Yel G, Akturk T. A new approach to (3+1) dimensional Boiti-Leon-Manna-Pempinelli equation. Appl Math Nonlinear Sci 2020;5(1):309–16.
[72] Akganduller O, Atmaca SP. Discrete normal vector field approximation via time scale calculus. Appl Math Nonlinear Sci 2020;5(1):349–60.
[73] Lanbaran NM, Celik E, Yigider M. Evaluation of investment opportunities with interval-valued fuzzy Topsis method. Appl Math Nonlinear Sci 2020;5(1):461–74.
[74] Hosseini K, Samavat M, Mirzazadeh M, Ma WX, Hammouch Z. A New (3+1)-dimensional Hirota Bilinear Equation: Its Bäcklund Transformation and Rational-type Solutions. Regular Chaotic Dyn 2020;25(4):383–91.
[75] Ozer O. A handy technique for fundamental unit in specific type of real quadratic fields. Appl Math Nonlinear Sci 2020;5(1):495–8.
[76] Dusunceli F. New Exact Solutions for Generalized (3+1) Shallow Water-Like (SWL) Equation. Appl Math Nonlinear Sci 2019;4(2):365–70.
[77] Ziane D, Cherif MH, Cattani C, Belghaba K. Yang-Laplace Decomposition Method for Nonlinear System of Local Fractional Partial Differential Equations. Appl Math Nonlinear Sci 2019;4(2):489–502.